

# Low-temperature sintering behavior of the nano-sized AlN powder achieved by super-fine grinding mill with Y<sub>2</sub>O<sub>3</sub> and CaO additives

Jin-Yu Qiu<sup>a</sup>, Yuji Hotta<sup>a</sup>, Koji Watari<sup>a,\*</sup>, Kenshi Mitsuishi<sup>b</sup>, Masato Yamazaki<sup>b</sup>

<sup>a</sup> *Advanced Sintering Technology Group, National Institute of Advanced Industrial Science and Technology, Shimoshidami, Moriyama-ku, Nagoya 463-8560, Japan*

<sup>b</sup> *Mitsui Chemicals, Shiodome City Center, Higashi-Shimbashi, Minato-ku, Tokyo 105-7117, Japan*

Available online 1 August 2005

## Abstract

For low-temperature sintering, mixtures of AlN powder doped with 3.53 mass% Y<sub>2</sub>O<sub>3</sub> and 0–2.0 mass% CaO as sintering additives were pulverized and dispersed in a vertical super-fine grinding mill with very small ZrO<sub>2</sub> beads. The particle sizes achieved ranged between 50 and 100 nm after grinding for 90 min. The mixtures were then fired at 1000–1500 °C for 0–6 h under nitrogen gas pressure of 0.1 MPa. All nano-sized powders showed pronounced densification from 1300 °C as revealed by shrinkage measurement. The larger amounts of sintering additives enhanced AlN sintering at lower temperatures. Densified AlN ceramics with very fine and uniform grains of 0.3–0.4 μm were obtained at a firing temperature of 1500 °C for 6 h.

© 2005 Elsevier Ltd. All rights reserved.

**Keywords:** A. Milling; A. Sintering; B. Grain size; Aluminum nitride (AlN)

## 1. Introduction

AlN ceramics have been used for substrates, packaging materials for high power integrated circuits for electronic devices, refractive materials in the metallurgical industry and so on.<sup>1–3</sup> However, due to its high covalent bonding, it is difficult to achieve solid-state sintering without using submicrometer powders or high pressures.<sup>3</sup> Liquid-phase sintering can be carried out to produce densified AlN ceramics. The most common additives are rare-earth and/or alkaline earth oxides,<sup>4,5</sup> which react with Al<sub>2</sub>O<sub>3</sub> on the surface of AlN powders during sintering. The additives not only form a liquid phase to enhance densification, but also improve the thermal conductivity by eliminating the oxygen from the AlN lattice.<sup>6,7</sup> In addition, the sinterability of AlN compacts is strongly dependent on size of starting powders. Nano-sized particles have shown potential for low-temperature sintering. Hashimoto et al.<sup>8</sup> and Panchula et al.<sup>9</sup> demonstrated that

close to theoretical densities could be obtained by pressureless sintering at 1700 °C using nano-sized powders. Although nano-sized powders possess intrinsic good sintering properties and nano-sized AlN powders have been successively synthesized,<sup>10–23</sup> these powders have a tendency to form agglomerations which result in poor sinterability. So the sintering temperatures also dwell above 1700 °C.<sup>9,10,24</sup>

On the other hand, coarse powders can be made smaller and more homogeneous by grinding. Conventional grinding methods, however, such as ball-milling or planetary milling, are only effective down to certain sizes. In a previous experiment,<sup>25</sup> an attempt was made to pulverize AlN powder with a primary particle size of 0.2 μm, which agglomerate size ranged from 0.5 to 1.0 μm, by planetary milling and ultrasonic vibration; however, the size and shape of agglomerations showed no significant changes. In the present paper, we describe a new process for pulverizing and dispersing AlN agglomerate powder doped with sintering aids by using very small mill media. Our main purpose is to demonstrate that nano-sized particles from well-ground and dispersed AlN powder possess good sinterability even under low-temperature sintering.

\* Corresponding author. Tel.: +81 52 736 7153; fax: +81 52 736 7405.

E-mail addresses: [jinyu-qiu@aist.go.jp](mailto:jinyu-qiu@aist.go.jp) (J.-Y. Qiu), [koji-watari@aist.go.jp](mailto:koji-watari@aist.go.jp) (K. Watari).

Table 1  
Compositions of the various AlN–Y<sub>2</sub>O<sub>3</sub>–CaO powder mixtures

NO	AlN (mass%)	Y <sub>2</sub> O <sub>3</sub> (mass%)	CaO (mass%)
AYC0	96.47	3.53	0
AYC1	95.47	3.53	1.0
AYC2	94.47	3.53	2.0

## 2. Experimental

High purity AlN powder (MAN-10, Mitsui Chemicals, Tokyo, Japan, primary particle size: 0.2 μm, specific surface area: 10 m<sup>2</sup>/g, oxygen content: 1.03 mass%), originally synthesized by vapor phase reaction between Al(C<sub>2</sub>H<sub>5</sub>)<sub>3</sub> and NH<sub>3</sub> as the starting material, was used in this study. 3.53 mass% Y<sub>2</sub>O<sub>3</sub> powder (purity 99.99%, Hokko Chemicals, Tokyo, Japan) and 0–2.0 mass% CaO powder were doped into the AlN powder as sintering additives. CaO was added in the form of CaCO<sub>3</sub> (purity 99.5%, Wako Pure Chemical Industries, Osaka, Japan). The compositions of the mixtures are listed in Table 1. One hundred grams of these mixtures and 900 ml of isopropyl alcohol solvent were mixed and the slurries pulverized and dispersed in a vertical super-fine grinding mill (UAM-015, Kotobuki Eng. & Mfg. Co. Ltd., Japan) using ZrO<sub>2</sub> beads 0.1 mm in diameter as the mill media and ground for 90 min. An agitation speed of 4000 rpm was used to exert both shearing and imparting forces on the AlN agglomerate particles. After drying, the granules were uniaxially pressed at 10 MPa in a steel die to make pellets. The pellets were cold isostatically pressed (CIP'ed) under 300 MPa for 120 s. The specimens were then placed into a BN crucible and sintered at 1000–1500 °C for 0–6 h in flowing nitrogen gas.

The shrinkages and densities of the specimens were measured using vernier caliper along the diameter of the sintered pellets<sup>26</sup> and the Archimedes method, respectively. The particle size distributions of the mixtures were measured using a laser diffraction particle size analyzer (LA-920, Horiba, Japan). The ground powders were observed by scanning electron microscopy (SEM, JSM-5600N, Jeol, Tokyo, Japan) and transmission electron microscopy (TEM, JEM 2010, Jeol Ltd.). The fracture surfaces of the samples were also

observed by SEM. The crystalline phases were analyzed by X-ray diffraction analysis (XRD, RINT-2000, Rigaku Corp., Japan).

## 3. Results and discussion

### 3.1. Pulverization and dispersion of the agglomerated AlN mixtures

Fig. 1 shows the particle size distributions of the raw and the mixture of AlN powder doped with 3.53 mass% Y<sub>2</sub>O<sub>3</sub> (AYC0 mixture) after grinding for 90 min. Their SEM photographs are shown in Fig. 2. The raw powder contained a significant proportion of particles with over 1.0 μm, and a wider particle size distribution. The mean particle size was 0.38 μm. The agglomerate particles had sizes ranging from 0.5 to 1.5 μm before grinding. As a result of the grinding process, powders or strongly coagulated agglomerates were sheared between small, hard-material ZrO<sub>2</sub> beads which were forced to stir in a limited volume, resulting in stronger grinding efficiency. The agglomerates were broken apart into very small particles. Fig. 1(b) shows that the size distribution shifted to the small end and became narrower and the fraction of larger particles, over 1.0 μm in size decreased drastically after grinding. The mean particle size was reduced to about 0.14 μm after grinding. The particles approached the nano scale, and showed a narrow particle size distribution. From SEM observation, we found that the particle sizes were homogeneous, suggesting that super-fine grinding is an efficient method for pulverization and dispersion of the agglomerate AlN mixtures, and the final powder became homogeneous and finer than that of their primary particles. Fig. 3 shows the TEM micrograph of the AYC0 mixture after grinding for 90 min. It indicates that the sizes of individual particle ranged between 50 and 100 nm.

The phase of well-ground powder was detected by XRD. AlN and Y<sub>2</sub>O<sub>3</sub> were identified as the major and minor crystalline phases, respectively. No traces of ZrO<sub>2</sub> were detected. The final particles produced an extensive broadening of the diffraction peaks and a decrease in X-ray intensities. The crystalline size of finely ground AlN powder was calculated

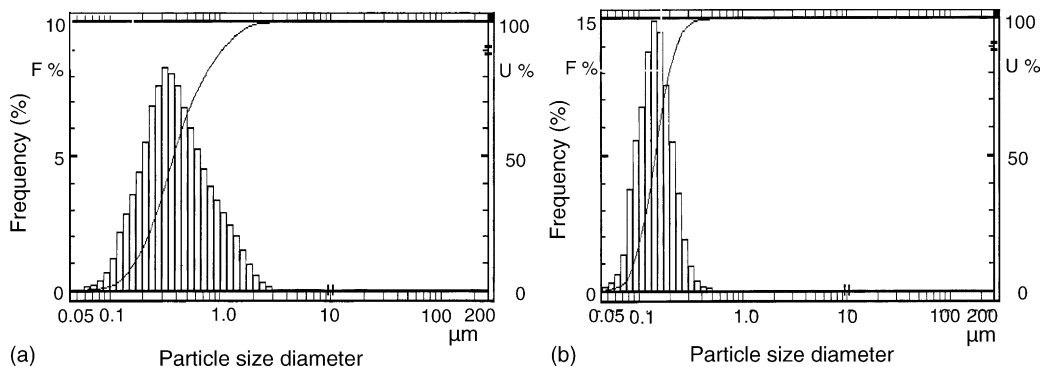


Fig. 1. The particle-size distribution after grinding for 90 min of (a) the raw AlN powder and (b) with 3.53 mass% Y<sub>2</sub>O<sub>3</sub> addition (AYC0).

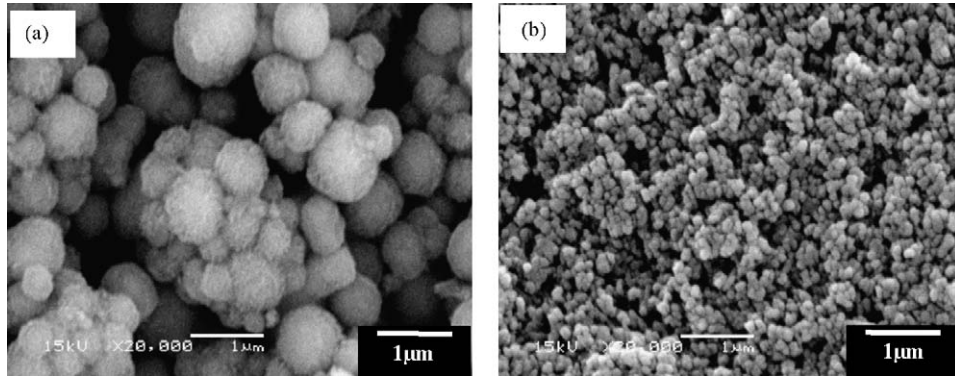


Fig. 2. SEM photographs of (a) the raw AlN powder before grinding and (b) with 3.53 mass%  $Y_2O_3$  addition (AYC0) after grinding for 90 min.

using Scherer’s Equation with XRD peak intensities,<sup>27</sup> and was estimated to be about 120 nm, which was in accordance with observations from the measurements by the laser diffraction particle size analyzer and TEM observation.

3.2. Sintering characteristics

The shrinkage behaviors of the specimens with 3.53 mass%  $Y_2O_3$  and various amounts of CaO addition are shown in Fig. 4. For well-ground powder with  $Y_2O_3$  and CaO sintering additions, marked shrinkages occurred at temperatures above 1300 °C in all cases. For comparison the sintering shrinkage curves of the agglomerated powder, the sintering shrinkage curve line of the agglomerate MAN-12 powder (specific surface area: 12 m<sup>2</sup>/g) doped with 5.2 mass%  $Y_2O_3$ <sup>25</sup> is also shown in Fig. 4. Its shrinkage is considerably lower than that using well-ground AlN powder at the range of 1300–1500 °C. It is clearly indicated that sintering of the nano-sized AlN powder prepared by the super-fine grinding mill stimulated densification at lower sintering temperatures. It was also observed that the shrinkage of sintered specimens increased with increasing amount of

CaO content at the initial stage of sintering. The different shrinkages of the fired samples with  $Y_2O_3$  and CaO additions were most likely attributable to the effects of the sintering additives on the liquid phases during the various sintering temperatures.<sup>26</sup> Doping with CaO increases the amount of liquid phase, resulting in enhanced densification. Finally, the shrinkages tended to be the same value at a sintering temperature of 1500 °C for 6 h. The total shrinkage was about 20% for all the densified samples.

The sinterability of the nanocrystalline AlN with 4.0 mass% nanocrystalline  $Y_2O_3$  as a sintering aid has been investigated by Panchula et al.<sup>9</sup> They reported that the density of the sintered sample reached  $\approx 95\%$  of the theoretical density at 1550 °C, but it did not further improve above this temperature. This is because that the  $Y_2O_3$  agglomerates prevented from the densification of AlN ceramics. As mentioned above, the mixtures of AlN with  $Y_2O_3$  and CaO sintering additions were milled together through super-fine grinding mill in our process. This suggested that the mixing of raw AlN and additions could be dispersed homogeneously by this novel process. According to the XRD patterns, ZrN was detected as one of the secondary phases, suggesting that amorphous  $ZrO_2$  contamination from the beads reacted with AlN and was converted to ZrN at high temperatures in the nitrogen gas.<sup>28,29</sup> The formations of ZrN phase are described

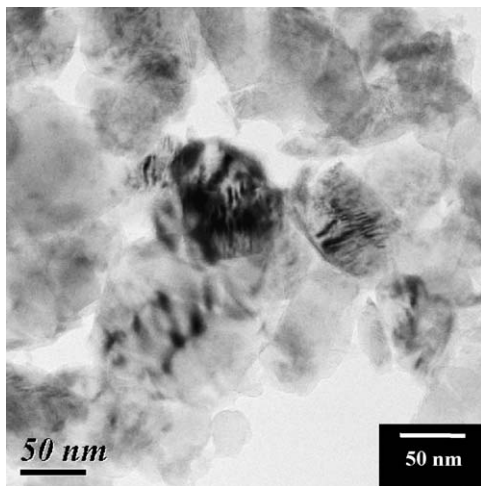


Fig. 3. TEM micrograph the mixture of AlN powder with 3.53 mass%  $Y_2O_3$  addition (AYC0) after grinding for 90 min.

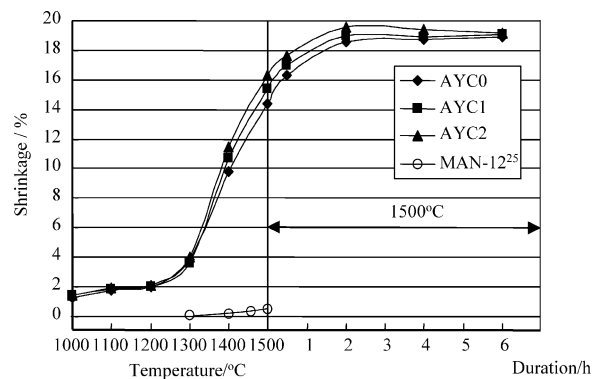


Fig. 4. The shrinkages of the specimens at firing temperatures between 1000 and 1500 °C and at 1500 °C for various duration.

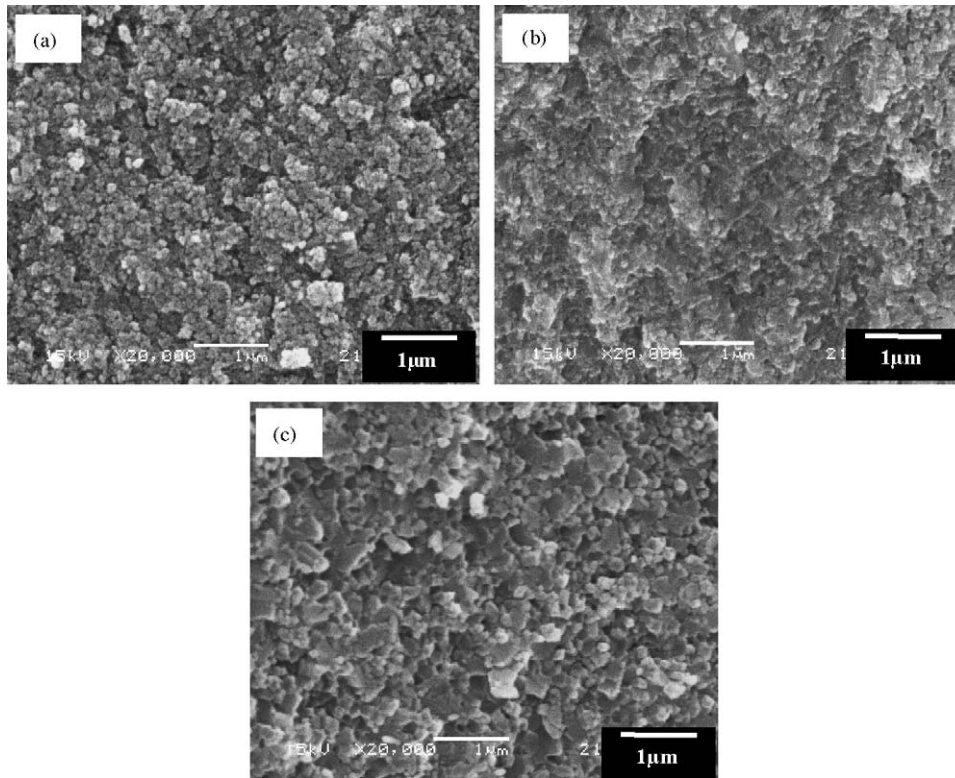


Fig. 5. SEM photographs of the AYC0 mixture sintered (a) at 1400°C for 0 h; (b) at 1500°C for 0 h and (c) at 1500°C for 2 h.

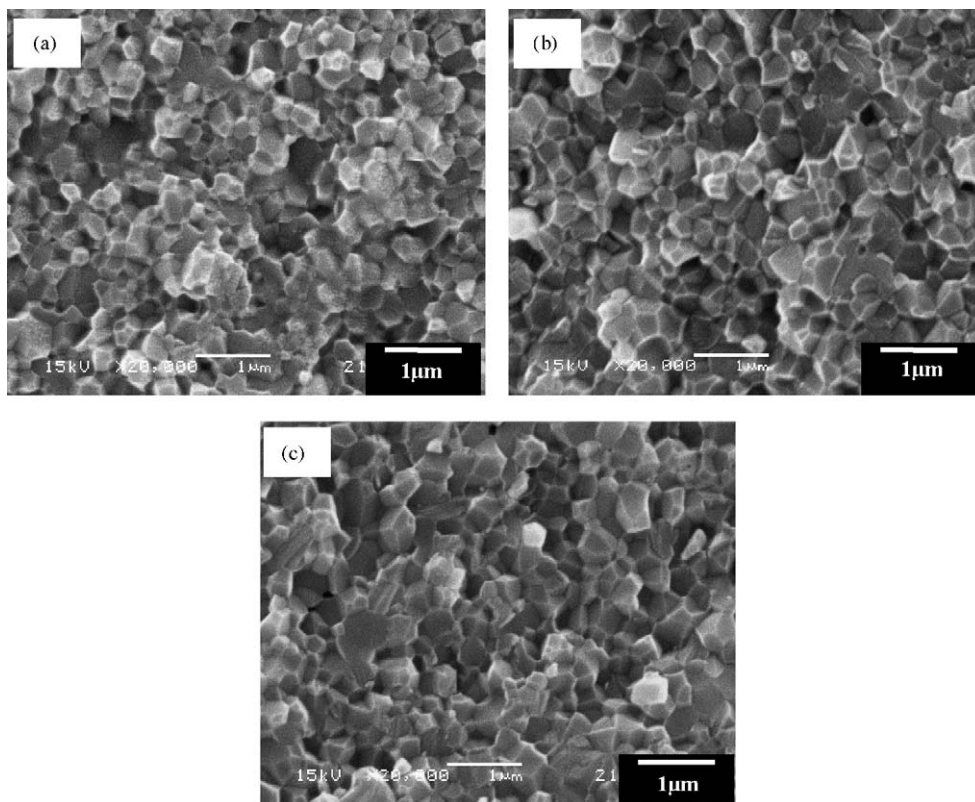


Fig. 6. SEM micrographs of (a) the AYC0 mixture; (b) the AYC1 mixture and (c) the AYC2 mixture sintered at 1500°C for 6h.



by reactions (1) and (2) below. The densities of AYC0, AYC1 and AYC2 were 3.39, 3.42 and 3.40 g/cm<sup>3</sup> after firing at 1500 °C for 6 h, respectively. These values exceeded the theoretical density of AlN (3.26 g/cm<sup>3</sup>) is due to the density of ZrN (7.29 g/cm<sup>3</sup>).

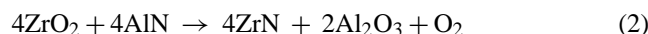
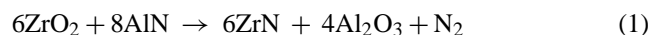


Fig. 5 shows SEM photographs of fracture surfaces of the AYC0 specimen sintered at 1400 °C for 0 h and 1500 °C for 2 h. The pulverized and dispersed mixtures did not re-agglomerate. Neck formation was observed at 1400 °C; the particles in the fired sample showed grains grew slightly. The pores in the specimen were subsequently reduced; some grains grew and contiguity of the particles increased during further sintering at 1500 °C. Grain growth and densification proceeded while soaking at 1500 °C for 2 h, but the grain boundaries were not very clear.

Fig. 6 comprises SEM photographs of fracture surfaces of the AYC0, AYC1 and AYC2 specimens sintered at 1500 °C for 6 h. The microstructures of all the samples showed no residual porosity and exhibited equiaxed and homogenous grains. This is fully consistent with the measured values for the densities. The densification process of AlN ceramics was promoted by liquid-phase sintering while using sintering additives, accompanying solution-reprecipitation between AlN and the liquid phase which affected the final AlN densities.<sup>4</sup> A comparison of Fig. 6(a) with Fig. 5(c) shows that with increased holding time, grains in the sintered sample AYC0 grew slightly, porosity reduced and the edges of grains became more distinct. This implies that reprecipitation was promoted during firing at 1500 °C for 6 h. Increasing the amount of sintering additions in Samples AYC1 and AYC2 appeared to lead to several small grains joining together and the grain boundaries between them becoming slightly more indistinct.

In our process, it was evident that after low-temperature sintering, fully dense structures were comprised of very fine grains with sizes of 0.3–0.4 μm, and is less than that of conventional AlN ceramics due to sintering temperatures above 1700 °C, resulting in rapid grain growth.<sup>9,10,24</sup> The fine microstructures are also expected to show improved mechanical strength. The results will be reported in our future work.

#### 4. Conclusions

Relatively coarse, agglomerated AlN powder can be made homogeneous and pulverized beyond traditional grain size limits by using the super-fine grinding mill with very small beads. The significant advantages of this process are that the ground particle size exceeds the conventional grinding limit, and yields very fine and homogenous particles. The sintering temperature of these mixtures was reduced to 1500 °C, which was 200 °C lower than that for conventional liquid-phase

sintering. Fully densified specimens were achieved after a holding time of 6 h. The investigation of the microstructures showed uniform grains with a size of 0.3–0.4 μm. Very small grain size AlN ceramic obtained by low-temperature sintering will meet the requirements for several new potential applications.

#### Acknowledgement

The authors are grateful to Dr. Hae-Weon Lee (KIST, Korea) for his valuable comments.

#### References

- Slack, G. A., Nonmetallic crystals with high thermal conductivity. *J. Phys. Chem. Solids*, 1973, **34**, 321–335.
- Werdecker, W. and Aldinger, F., Aluminum nitride—an alternative ceramics substrate for high-power application in microcircuit. *IEEE Trans. Comp., Hybrids, Manuf. Technol., CHMT-7*, 1984, 399–404.
- Sheppard, L. M., Aluminum nitride: a versatile but challenging material. *Am. Ceram. Bull.*, 1990, **69**, 1801–1812.
- Komeya, K., Tsuge, A. and Inoue, A., Effect of CaCO<sub>3</sub> addition on the sintering of AlN. *J. Mater. Sci. Lett.*, 1982, **1**, 325–326.
- Komeya, K., Inoue, H. and Tsuge, A., Effect of various additives on sintering of aluminum nitride. *Yogyo-Kyokaiishi*, 1985, **93**, 41–46.
- Shinozaki, K. and Tsuge, A., Development of high thermal conductivity AlN. *Ceramics (Bull. Ceram. Soc. Jpn.)*, 1986, **21**, 1130–1135.
- Virkar, A. F., Jackson, T. B. and Cutler, R. A., Thermodynamic and kinetic effect of oxygen removal on the thermal conductivity of aluminum nitride. *J. Am. Ceram. Soc.*, 1989, **72**, 2031–2042.
- Hashimoto, N., Yoden, H. and Deki, S., Sintering behavior of fine aluminum nitride powder synthesized from aluminum polynuclear complexes. *J. Am. Ceram. Soc.*, 1992, **75**(8), 2098–3106.
- Panchula, M. L. and Ying, J. Y., Nanocrystalline aluminum nitride. II. Sintering and properties. *J. Am. Ceram. Soc.*, 2003, **86**(7), 1121–1127.
- Lan, Y. C., Chen, X. L., Cao, Y. G., Xu, Y. P., Xun, L. D., Xu, T. et al., Low-temperature synthesis and photoluminescence of AlN. *J. Cryst. Growth*, 1999, **207**, 247–250.
- Cao, Y. G., Chen, X. L., Lan, Y. C., Li, J. Y., Xu, Y. P., Xu, T. Q. et al., Blue emission and raman scattering spectrum from AlN nanocrystalline powders. *J. Cryst. Growth*, 2000, **213**, 198–202.
- Park, J. R., Rhee, S. W. and Lee, K. H., Gas-phase synthesis of AlN powders from AlCl<sub>3</sub>–NH<sub>3</sub>–N<sub>2</sub>. *J. Mater. Sci.*, 1993, **28**, 57–64.
- Itatani, K., Sano, K., Howell, F. S., Kishioka, A. and Kinoshita, M., Some properties of aluminum nitride powder synthesized by low-pressure chemical vapour deposition. *J. Mater. Sci.*, 1993, **28**, 1631–1638.
- Pratsinis, S. E., Wang, G., Panda, S., Guiton, T. and Weimer, W., Aerosol synthesis of AlN by nitridation of aluminum vapor and clusters. *J. Mater. Res.*, 1995, **10**(3), 512–520.
- Moura, F. J. and Munz, R. J., Vapor-phase synthesis of nanosize aluminum nitride particles using a two-stage transferred arc reactor. *J. Am. Ceram. Soc.*, 1997, **80**(9), 2425–2428.
- Cruz, A. C. and Munz, R. J., Vapor phase synthesis of fine particles. *IEEE Trans. Plasma Sci.*, 1997, **25**(5), 1008–1016.
- David, M. S., Babu, V. and Rasmussen, B. H., RF plasma synthesis of amorphous AlN powder and films. *AIChE J.*, 1990, **36**(6), 871–876.
- Grigoriu, C., Hirai, M., Nishiura, K., Jiang, W. and Yatsui, K., Synthesis of nano-sized aluminum nitride powders by pulsed laser ablation. *J. Am. Ceram. Soc.*, 2000, **83**(10), 2631–2633.

19. Zhu, Q., Jiang, W. and Yatsui, K., Numerical and experimental studies on synthesis of ultrafine nanosize powders of AlN by ion beam evaporation. *J. Appl. Phys.*, 1999, **86**(9), 5279–5285.
20. Jiang, W. and Yatsui, K., Pulsed wire discharge for nanosize powder synthesis. *IEEE Trans. Plasma Sci.*, 1998, **26**(5), 1498–1501.
21. Panchula, M. L. and Ying, J. Y., Nanocrystalline aluminum nitride. I. Vapor-phase synthesis in a forced-flow reactor. *J. Am. Ceram. Soc.*, 2003, **86**(7), 1114–1120.
22. Qiu, Y. and Gao, L., Novel way to synthesize nanocrystalline aluminum nitride from coarse aluminum powder. *J. Am. Ceram. Soc.*, 2003, **86**(7), 1214–1216.
23. Suehiro, T., Hirosaki, N., Terao, R., Tatami, J., Meguro, T. and Komeya, K., Synthesis of aluminum nitride nanopowder by gas-reduction–nitridation method. *J. Am. Ceram. Soc.*, 2003, **86**, 1046–1048.
24. Suehiro, T., Hirosaki, N. and Komeya, K., Synthesis and sintering properties of aluminum nitride nanopowder prepared by the gas-reduction–nitridation method. *Nanotechnology*, 2003, **14**, 487–491.
25. Watari, K., Brito, M. E., Yasuoka, M., Valecillos, M. C. and Kanzaki, S., Influence of powder characteristics on sintering process and thermal conductivity of aluminum nitride ceramics. *J. Ceram. Soc. Jpn.*, 1995, **103**(9), 891–990.
26. Qiao, L., Zhou, H., Xue, H. and Wang, S., Effect of Y<sub>2</sub>O<sub>3</sub> on the low temperature sintering and thermal conductivity of AlN ceramics. *J. Eur. Ceram. Soc.*, 2003, **23**, 61–67.
27. Klug, H. and Alexander, L., *X-ray Diffraction Procedures for Polycrystalline Amorphous Materials*. Wiley, New York, 1974, pp. 618–708.
28. Mukerji, J., Stabilization of cubic zirconia by aluminum nitride. *J. Am. Ceram. Soc.*, 1989, **72**(8), 1567–1568.
29. Kosori, M., Ueno, F. and Tsuge, A., Effects of transition-metal additions on the properties of AlN. *J. Am. Ceram. Soc.*, 1994, **77**(8), 1991–2000.